

## FLUID-STRUCTURE INTERACTION OF BODY WITH ELASTIC WALL

Esmatullah Maiwand Sharify<sup>\*</sup>, Norio Arai<sup>†</sup>, and Shun Takahashi<sup>††</sup>

<sup>\*</sup>Dept. of Mech. Sys. Eng., Tokyo University of Agriculture and Technology  
(TUAT), Koganei, Tokyo, Japan 184-8588  
e-mail: [esmat.maiwand@gmail.com](mailto:esmat.maiwand@gmail.com)

[arai@cc.tuat.ac.jp](mailto:arai@cc.tuat.ac.jp)

[takahass@cc.tuat.ac.jp](mailto:takahass@cc.tuat.ac.jp)

**Key words:** Fluid Structure Interaction, Numerical Simulation, Elastic Wall, Body Oscillation, Circular Cylinder

***Abstract.** This research is devoted to a numerical study of fluid-structure interaction problems, such kind of problems can be observed in many industrial and engineering applications. This research discusses the oscillatory characteristics of the elastic bodies and the flowfield around an isolated circular cylinder and two circular cylinders arranged in tandem at Reynolds number, 1000. Cylinders are simulated as rigid bodies and elastic bodies, respectively. The objective is to clarify the behaviors of the flowfield and elastic wall to control the bodies' vibration characteristics in unsteady flows. As a result, it is obtained that usage of the elastic wall on isolated circular cylinder shows some significant effects on vibration characteristics, in particular when the cylinder is allowed to oscillate in arbitrary direction and in the case of double cylinders the effect of elastic surface is significant on the downstream cylinder in static case. When the cylinders are allowed to oscillate in arbitrary direction, the effect of elastic surfaces on vibration characteristics are dominant on upstream cylinder as well as downstream cylinder.*

## 1 INTRODUCTION

Fluid Structure Interaction (FSI) occurs where fluid flow exerts pressure on a solid structure that may cause the structure to deform or move, such that it perturbs the uniform fluid flow. The dynamic interaction between a fluid and a structure is a mechanism that is ruled by several disciplines of physics. It may lead to very complicated problems including fluid dynamics, solid mechanics and vibration. One common form of FSI is the vortex-induced vibration (VIV). VIV plays an important role in many industrial and engineering applications such as aerospace engineering, civil engineering, biomedical engineering, marine engineering, etc. There for, numerous studies have been carried out to investigate about them. In this field, a circular cylinder forms the basic component of structures. And accordingly a considerable attention has been paid for flow around a circular cylinder as well as a pair of circular cylinders.

VIV is a direct consequence of lift and drag oscillations due to the vortex shedding. When the bluff body is placed in uniform flow, the attached flow separates from the surface of the body, and vortices are generated in the wake. The vortex motion in the vicinity of the bodies exerts periodic influence on them. As a result, the vortex induces vibrations. When the frequency of vortex shedding coincides with the structural natural frequency, the VIV can occur with high amplitudes that may cause damage to the structure. The aim of this work is to clarify the behaviors of the flowfield and elastic wall to control the bodies' vibration characteristics in unsteady flow.

## 2 METHODOLOGY

### 2.1 Governing equations

Flows investigated in this paper are calculated using the continuity equation and the Navier-Stokes equations. The Poisson equation for the pressure is derived by the divergence operation of the Navier-Stokes equations

$$\text{div } \mathbf{u} = 0 \quad (2.1)$$

$$\frac{\partial \mathbf{u}}{\partial t} + (\mathbf{u} \cdot \text{grad}) \mathbf{u} = -\text{grad } p + \frac{1}{\text{Re}} \nabla^2 \mathbf{u} \quad (2.2)$$

$$\nabla^2 p = -\text{div}[(\mathbf{u} \cdot \text{grad}) \mathbf{u}] + R \quad (2.3)$$

Where

$$R = -\frac{\partial D}{\partial t} + \frac{1}{\text{Re}} \nabla^2 D, \quad D \equiv \text{div } \mathbf{u} \quad (2.4)$$

Finally the velocity at a certain time can be obtained from the Navier-Stokes equations and the pressure can be solved by Poisson equation.

The convective term of Navier-Stokes equations is discretized by the third-order upwind Kawamura-Kuwahara scheme1) (equation 2.5), while the second-order central difference scheme3) is adopted for the other terms and the discretized equations are solved by the SOR (Successive over-relaxation) method.

$$\left( \mathbf{u} \frac{\partial \mathbf{u}}{\partial x} \right) \approx \mathbf{u}_k \frac{-\mathbf{u}_{k+2} + 8(\mathbf{u}_{k+1} - \mathbf{u}_{k-1}) + \mathbf{u}_{k-2}}{12\Delta x} + \alpha |\mathbf{u}_k| \frac{\mathbf{u}_{k+2} - 4\mathbf{u}_{k+1} + 6\mathbf{u}_k - 4\mathbf{u}_{k-1} + \mathbf{u}_{k-2}}{12\Delta x} \quad (2.5)$$

By using the implicit Euler scheme, the Navier-Stokes equation takes following form:

$$\frac{\mathbf{u}^{n+1} - \mathbf{u}^n}{\Delta t} + ((\mathbf{u}^{n+1} - \mathbf{X}_t) \cdot \text{grad}) \mathbf{u}^{n+1} = -\text{grad}p + \frac{1}{\text{Re}} \nabla^2 \mathbf{u}^{n+1} \quad (2.6)$$

The the convective term is linearized for  $\mathbf{u}^{n+1}$  as follow:

$$(\mathbf{u}^{n+1} \cdot \text{grad}) \mathbf{u}^{n+1} \approx (\mathbf{u}^n \cdot \text{grad}) \mathbf{u}^{n+1} \quad (2.7)$$

## 2.2 Coordinate transformations

In this study a boundary-fitted coordinate system is applied, accordingly fine grid scale is provided near the cylinder wall. The numbers of grid points are as follows:

Single cylinder:  $i_{\max} \times j_{\max} = 97 \times 110$

Two cylinders in tandem:  $i_{\max} \times j_{\max} = 271 \times 105$

## 2.3 Boundary conditions

The boundary conditions are used as follows:

Velocity:

(i) Uniform flow at the in-flow boundary

$$u = 1, v = 0 \quad (2.8)$$

(ii) The fluid velocity is zero on the surface

$$u = 0, v = 0 \quad (2.9)$$

(iii) Uniform flow at infinity except for the downstream boundary

$$u = 1, v = 0 \quad (2.10)$$

(iv) Non-reflecting Sommerfeld boundary condition<sup>6)</sup> at the downstream boundary

$$\frac{\partial u}{\partial t} + U \frac{\partial u}{\partial x} = 0 \quad (2.11)$$

$$\frac{\partial v}{\partial t} + U \frac{\partial v}{\partial x} = 0 \quad (2.12)$$

Pressure:

(i) In-flow boundary:

$$p = 0 \quad (2.13)$$

(ii) On the surface:

For the object in the oscillating case, following method is used for pressure on the body<sup>7)</sup>:

$$p_\eta = -(x_\eta u_\tau + y_\eta v_\tau) \quad (2.14)$$

(iii) On the downstream boundary:

$$p = 0 \quad (2.15)$$

## 2.4 Body motion equation

The motion equation of oscillating cylinder can be described by

$$\frac{d^2\mathbf{S}}{dt^2} + 2\zeta\omega_n \frac{d\mathbf{S}}{dt} + \omega_n^2\mathbf{S} = \frac{\mathbf{F}(t)}{m} \quad (2.16)$$

$$\zeta = \frac{c}{2\sqrt{mk}}, \quad \omega_n = \sqrt{\frac{k}{m}} = 2\pi f_n$$

In this study we assume the damping factor of oscillating cylinder as “zero” ( $\zeta = 0$ ). The natural frequency is selected as  $f_n = 0.38$  Hz, 0.12 Hz for single cylinder and two cylinders in tandem, respectively according to previous studies<sup>9)</sup> and the work which has already done by us.

## 2.5 Flexible wall model

In this study the elastic wall is treated by the mass spring-force model in the uniform flow as shown in figure 2.1. Thus, the motion of the elastic wall can be described by equation (2.17).

$$\frac{d^2\mathbf{S}_{wall}^i}{dt^2} + 2\zeta_{wall}\omega_{nwall} \frac{d\mathbf{S}_{wall}^i}{dt} + \omega_{nwall}^2\mathbf{S}_{wall}^i = \frac{\Delta s_{wall}^i \cdot \mathbf{P}^i(t)}{\Delta m_{wall}} \quad (2.17)$$

$$\zeta_{wall} = \frac{c_{wall}}{2\sqrt{\Delta m_{wall}k_{wall}}}, \quad \omega_{nwall} = \sqrt{\frac{k_{wall}}{\Delta m_{wall}}} = 2\pi f_{nwall}$$

Here superscript  $i$  shows grid points number on elastic wall,  $\mathbf{S}$  indicates displacement of elastic wall and each grid point on the object surface assumes as elastic wall.

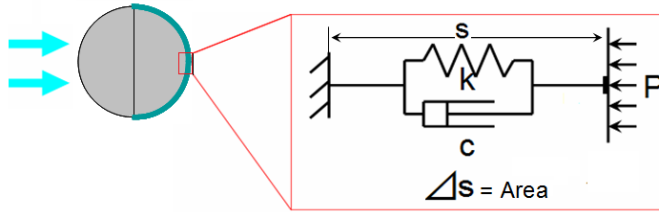


Figure 2.1: Elastic wall model.

This study deals with viscous fluid and the Reynolds number is based on the diameter of the cylinder, free-stream velocity and the viscosity of the fluid, so the kinematic viscosity of fluid is assumed  $\nu = 1.004 \times 10^{-6} \text{ m}^2/\text{s}$  and the diameter of cylinder is selected  $D = 0.05 \text{ m}$ .

The mass ratio is considered  $m' = 1.0$ , while time interval are assumed as  $\Delta t = 0.0005$ .

## 3 COMPUTATIONAL RESULTS

### 3.1 Single circular cylinder

Work in this section aims to investigate the flow around a circular cylinder at Reynolds number, 1000. The flowfield around cylinder (as rigid body and elastic body) is simulated both in stationary case and in oscillating case in arbitrary direction. Four points N, M, O and P are assumed as elastic points on the circumference of the cylinder to track the typical displacements of elastic movements. In this paper the expression of model A is used for rigid case, model B means that half back side of cylinder is

covered by elastic wall (rigid-front-flexible-rear) and the expression of model C stands for cylinder in which whole the surface of cylinder is considered as an elastic surface.

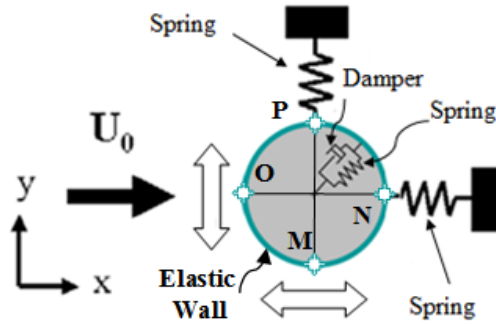
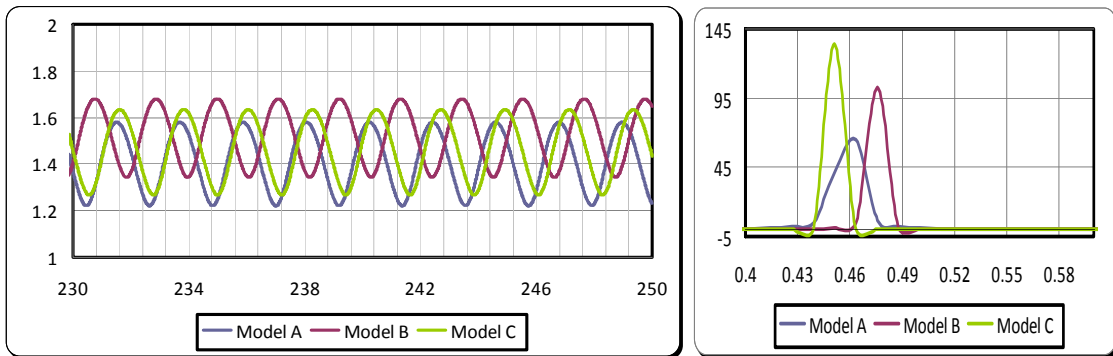


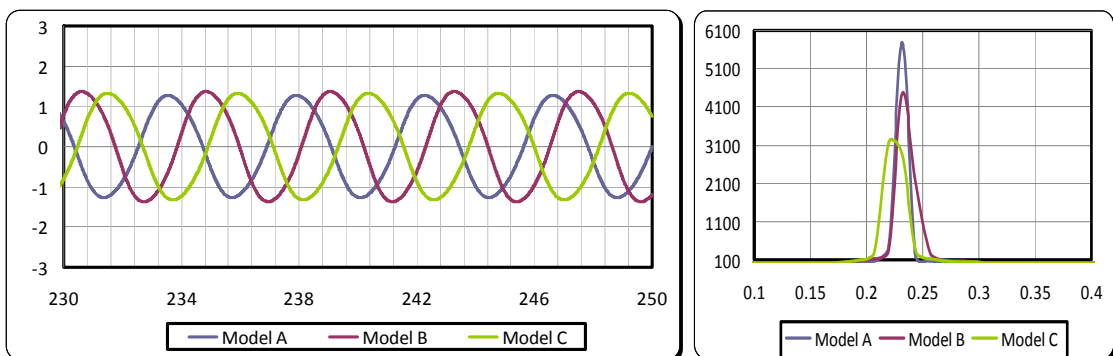
Figure 3.1: Schematic model for single cylinder oscillating in arbitrary direction (Model C).

It is obtained that the drag and lift coefficients and their frequencies are influenced by the effect of elastic wall. Fast Fourier Transform (FFT) is applied to drag and lift coefficient histories.

Figure 3.2 shows the comparison of drag and life coefficients and their power spectra for static cylinder in rigid and elastic cases.



(a) Drag coefficients history and their power spectra



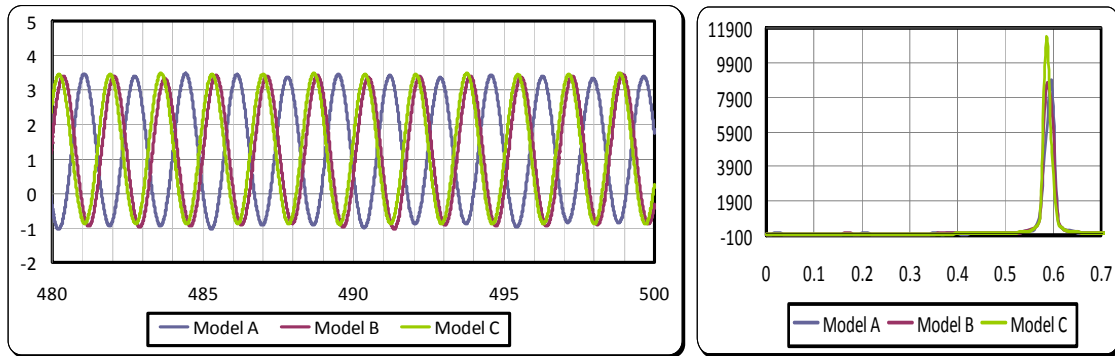
(a) Lift coefficients history and their power spectra

Figure 3.2: Drag and lift coefficients and their power spectra for rigid and elastic cylinder in static case.

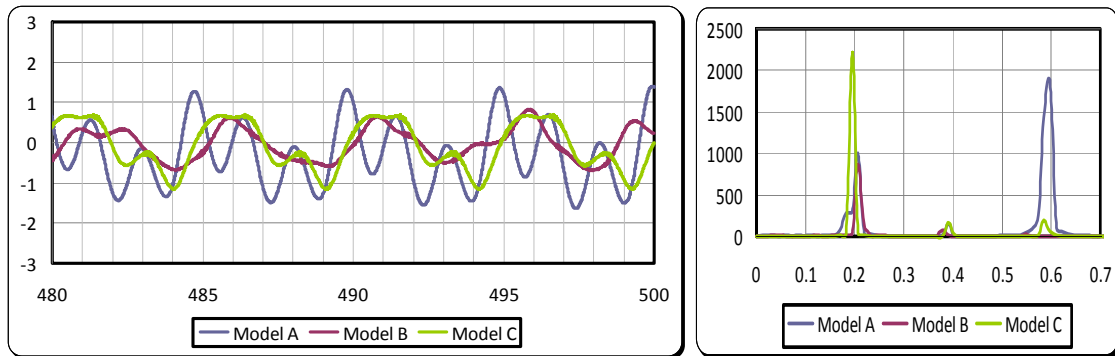
A separation point for circular cylinder usually moves and adjusts itself in response to the flow structure in the separation region<sup>4)</sup>. When the flow interacts the elastic

surface of the cylinder, the surface of the cylinder deforms. And as result, the passive deformation of the surface affects on separation point as well as vortex shedding frequency. In the single cylinder in static case, it is obtained that the effect of elastic surface for model B is bigger than model A and C. In the case of the model B, the surface deformation starting point makes small corner and effects on flow separation region. Therefore, the location of the flow separation point may become different compared to rigid and whole elastic cases.

Figure 3.3 shows the comparison of drag and lift coefficients for a cylinder oscillating in arbitrary direction in rigid and elastic conditions and their power spectra as well. It is observed that frequencies of drag coefficients for rigid and elastic (Model B and C) cases take place in same region, while frequencies of lift coefficients for elastic (Model B and C) cases, decrease significantly.



(a) Drag coefficients history and their power spectra



(a) Lift coefficients history and their power spectra

Figure 3.3: Drag and lift coefficients and their power spectra for rigid and elastic cylinder oscillating in arbitrary direction.

In this work, it is clarified that due to the implementation of elastic wall on the surface in static case, lift and drag coefficients increase around 4 and 8% for model B, respectively,. But in the case of cylinder oscillating in arbitrary direction, lift coefficient decrease around 31% for model B and 16 % for model C and also body oscillation amplitude is suppressed for model B and model C compared to model A.

<b>Single Cylinder, Static case</b>					
<b>Data</b>	<b>Model A</b>	<b>Model B</b>	<b>Model C</b>	<b><math>\Delta AB</math></b>	<b><math>\Delta AC</math></b>
<b>Cd(average)</b>	1.41	1.52	1.46	<b>8%</b>	<b>4%</b>
<b>Cl (rms)</b>	0.9	0.94	0.93	<b>4%</b>	<b>3%</b>
<b>Single Cylinder, Static case</b>					
<b>Data</b>	<b>Model A</b>	<b>Model B</b>	<b>Model C</b>	<b><math>\Delta AB</math></b>	<b><math>\Delta AC</math></b>
<b>Cd(average)</b>	1.22	1.2	1.28	<b>-2%</b>	<b>5%</b>
<b>Cl (rms)</b>	0.87	0.6	0.73	<b>-31%</b>	<b>-16%</b>

Table 3.1: Lift and drag coefficients for single cylinder in rigid and elastic cases.

In this section it can be observed that the cylinder vibrations are mainly in the inline direction. However, lock-in is not observed and the cylinder does not show large amplitude oscillations. It is necessary to visualize the computational solution and investigate the details of the flowfield near the wake region. Therefore, vorticity contours are drawn around the cylinder for static and oscillating in arbitrary direction in rigid and elastic cases. The vorticity fields at non-dimensional time  $t=239.5, 240.25, 241, 241.75, 242.5, 243.25, 244$  and  $244.75$  are shown for cylinder in static case. It is observed that the vortices are shedding from upper and lower side of the cylinder alternately.

When the circular cylinder is oscillating in arbitrary direction with natural frequency of 0.38Hz, the cylinder keeps disorganized motion during  $t=150\sim 200$ , after that, the vortex shedding becomes periodically during  $t=250\sim 300$ . Then, the flowfield are visualized at non dimensional time  $t=489.5, 490.25, 491, 491.75, 492.5, 493.25, 494$  and  $494.75$ . As a result, it is observed that twin vortices are shed from the cylinder in same time. The vortex size becomes smaller compared to the vortex that is generated around a cylinder in static case. During each cycle of shedding, another weak vortex is shed from the cylinder alternately from upper and lower surface of the cylinder in addition to a pair of vortices.

In this section it is investigated that the elastic surface is able to control passively the characteristic of vibrations. As a result, the frequencies for lift coefficient decreases and it causes to suppress the lift coefficients and the vibration amplitude in lateral direction as well. The phenomenon can be seen in flow visualization by vorticity, as shown in following figures.

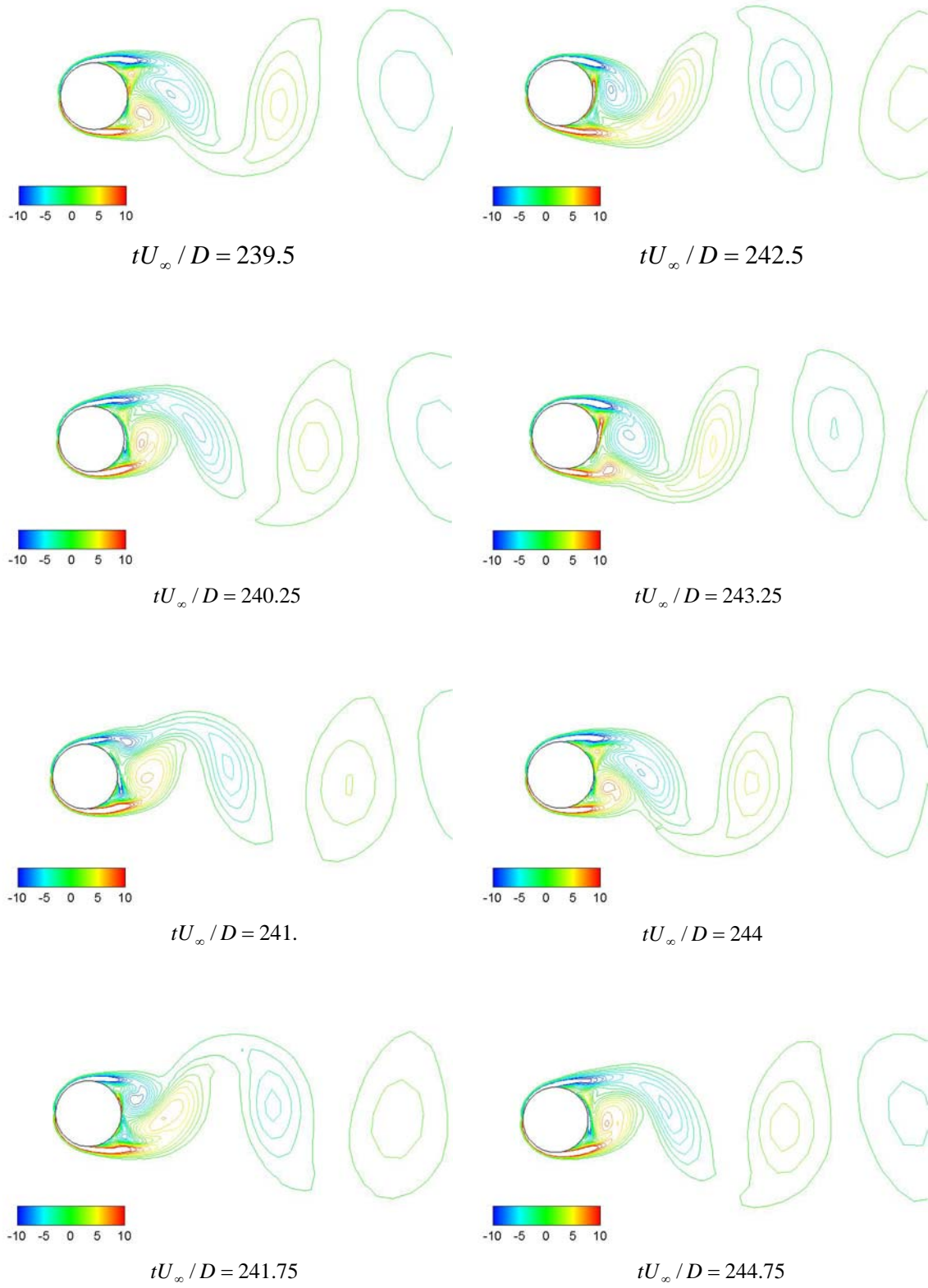


Figure 3.4: Instantaneous vorticity contours for single cylinder in static case (model A).



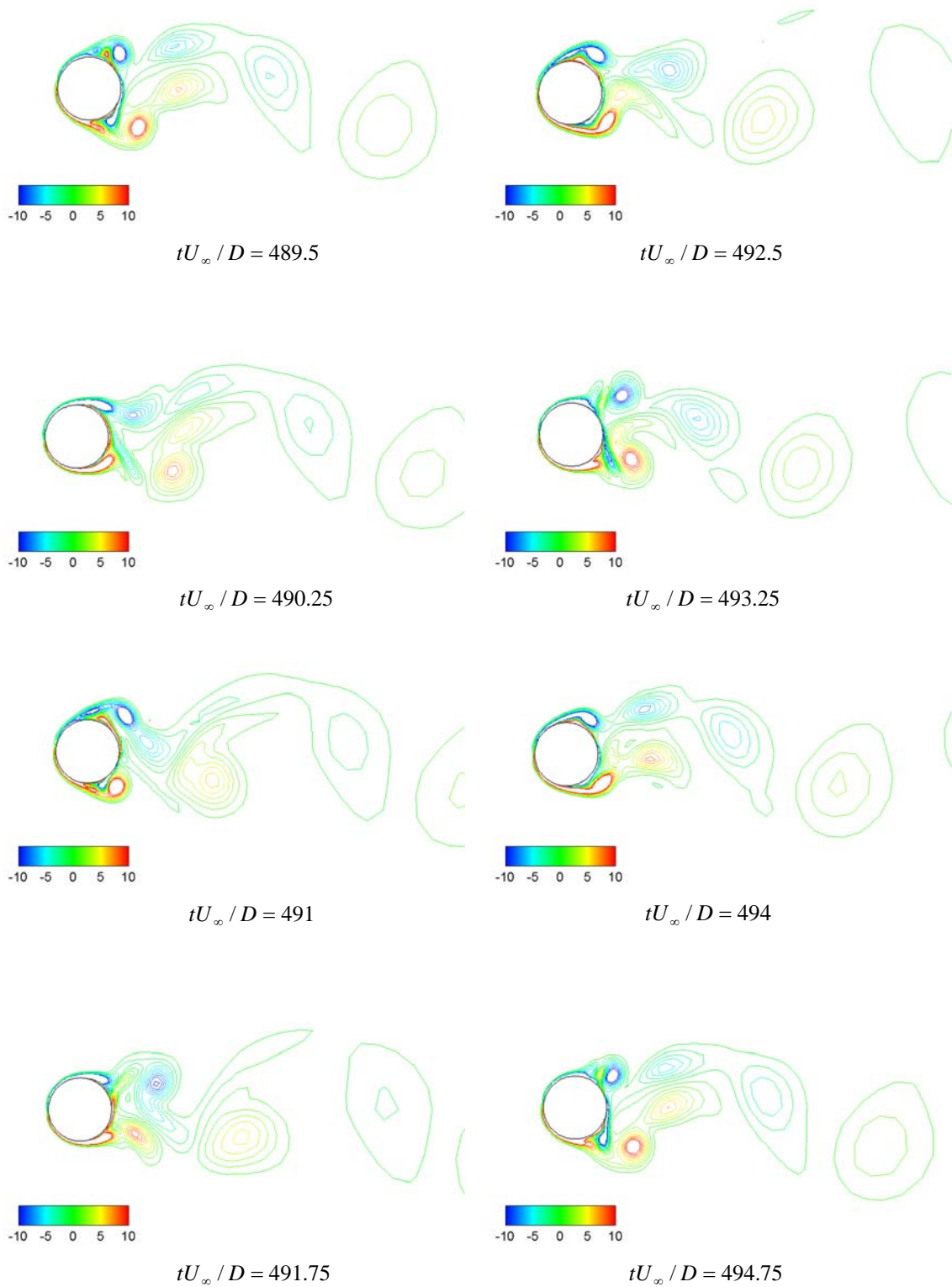


Figure 3.5: Instantaneous vorticity contours for single cylinder oscillating in arbitrary direction (modelA).

### 3.2 Two circular cylinders in tandem

This section is devoted to investigate the flow around a pair of equal-sized cylinders arranged in tandem at Reynolds number, 1000. The cylinders are set in streamwise direction by 1.5 times the cylinder diameter and analyzed as rigid bodies and elastic bodies, in stationary condition and oscillating condition in arbitrary direction. The flow around multiple bodies presents higher complicated phenomena than for a single body case. For two circular cylinders, the shear layer separated from the upstream cylinder reattaches onto the downstream cylinder.

Computational results of two cylinders in static and oscillating cases are compared with previous studies <sup>5 and 9)</sup>, then cylinders are treated with the elastic surface and compared with rigid case to ascertain the effect of elastic wall with respect to the vibration characteristics.

Here model D is used for rigid case (both upstream and downstream cylinders are rigid), the expression of model E means that half back side of upstream cylinder as well as half front side of downstream cylinder are considered as elastic surfaces and the expression of model F stands for arrangement of cylinders that whole circumferences, of downstream cylinder and upstream cylinder are treated by elastic surfaces. Eight points N, M, O, P, Q, R, S and T are assumed on the circumference of the cylinders to track the typical displacements of elastic walls.

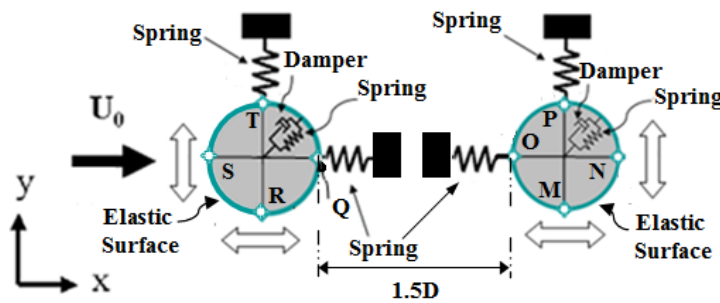
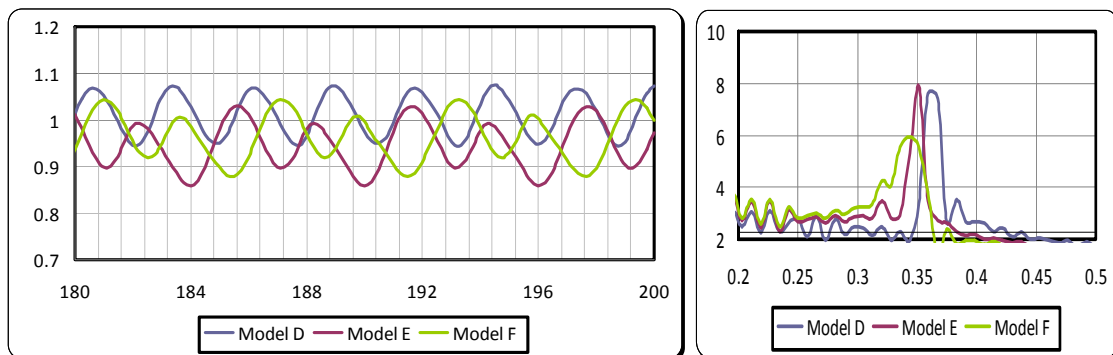
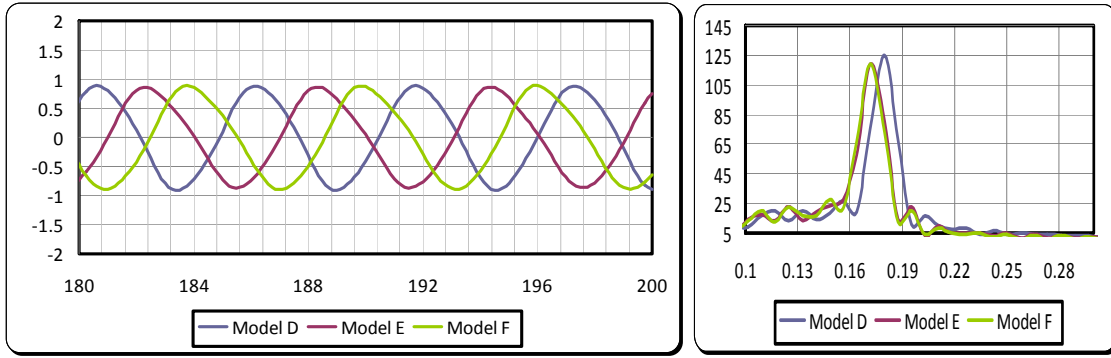


Figure: 3.6 Schematic model of two circular cylinders in tandem (Model F).

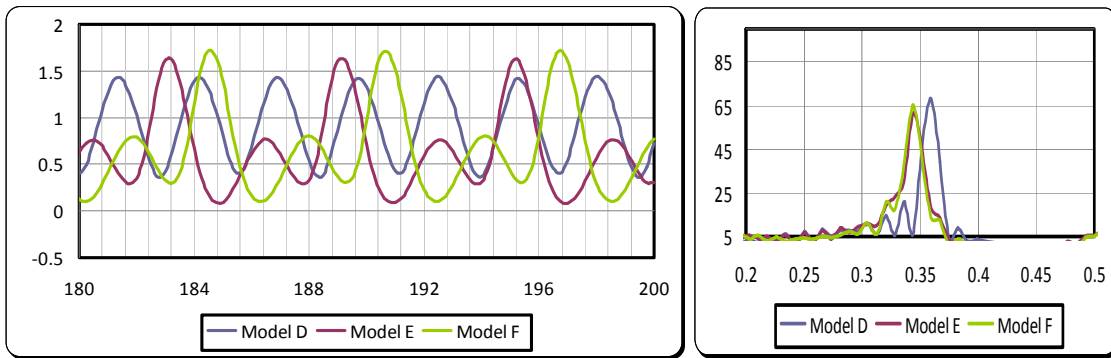
For the case of flows past two cylinders in stationary case, it is observed that the downstream cylinder lies in the wake of the upstream cylinder. Therefore it experiences large unsteady forces. But generally there is a decrease in the mean drag coefficient for both cylinders compared to single cylinder. The calculated lift and drag coefficients and their power spectra of both cylinders in rigid and elastic cases for static condition are shown in following drawings.



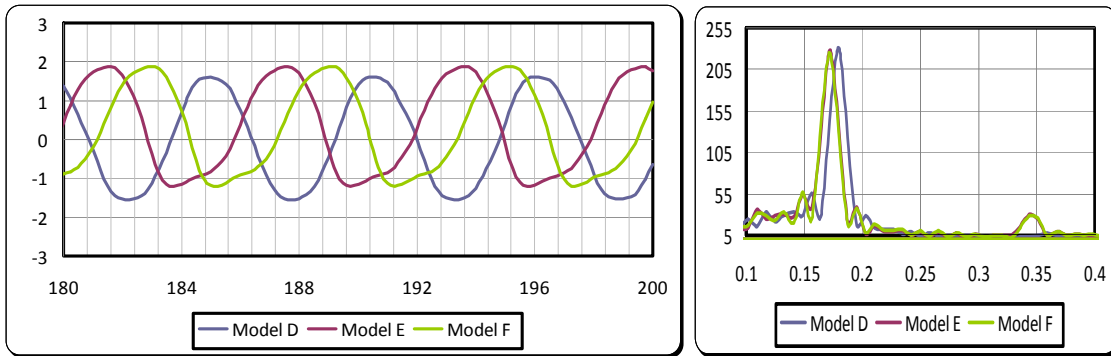
(a) Drag coefficients and their power spectra (upstream cylinder)



(b) Lift coefficients and their power spectra (upstream cylinder)



(c) Drag coefficients and their power spectra (downstream cylinder)



(d) Lift coefficients and their power spectra (downstream cylinder)

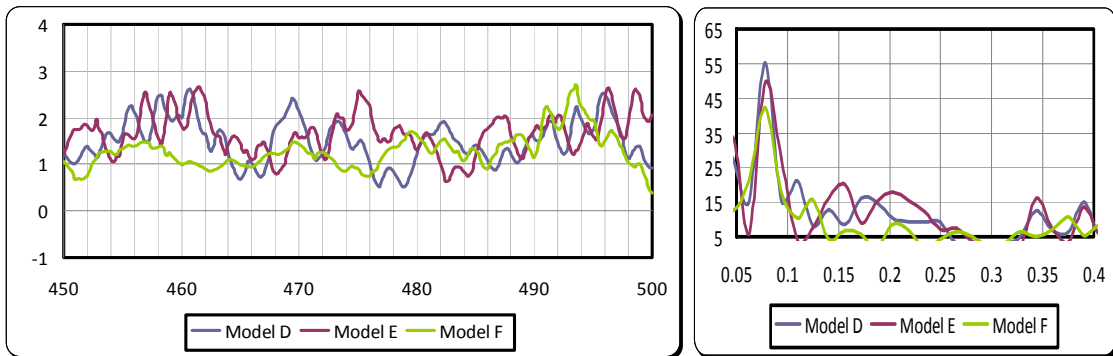
Figure 3.7: Comparison of  $C_d$ ,  $C_l$  and their power spectra of static upstream and downstream cylinders in rigid and elastic cases.

The effect of elastic surface for upstream cylinder is smaller in model E and model F compared to rigid model D case from the viewpoint of the mean value. On the other hand, the elastic surface has significant effect on downstream cylinder. Due to reaction of elastic surface the drag coefficient for downstream cylinder decrease around 27% in model E as well as 22% in model F, shown in Table 3.2.

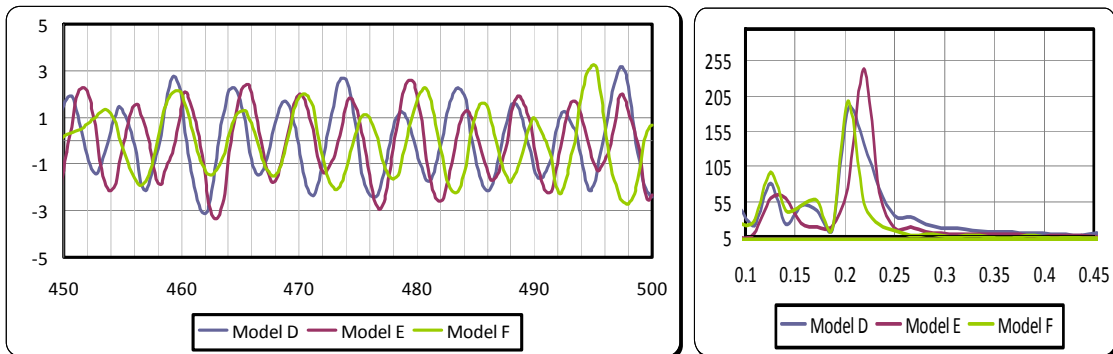
Two Cylinders in Tandem Arrangement, Stationary Case					
Upstream Cylinder					
Data	Model D	Model E	Model F	$\Delta DE$	$\Delta DF$
<b>Cd (average)</b>	1.01	0.96	0.97	<b>-5%</b>	<b>-4%</b>
<b>Cl (rms)</b>	0.75	0.73	0.75	<b>-3%</b>	<b>0%</b>
Downstream Cylinder					
Data	Model D	Model E	Model F	$\Delta DE$	$\Delta DF$
<b>Cd (average)</b>	0.92	0.67	0.72	<b>-27%</b>	<b>-22%</b>
<b>Cl (rms)</b>	1.03	1.03	1.02	<b>0%</b>	<b>-1%</b>

Table 3.2: Lift and drag coefficients of upstream and downstream cylinders in stationary case.

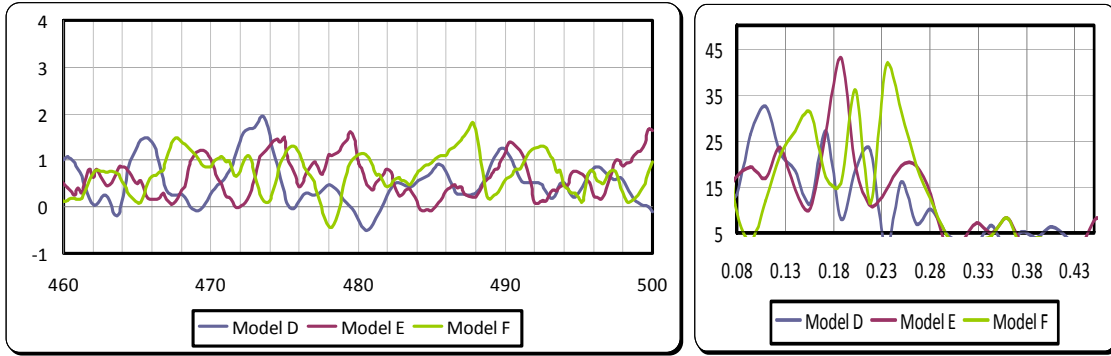
When cylinders are oscillated in arbitrary direction, it is observed that the upstream cylinder exhibits larger amplitude oscillations than downstream cylinder. Although the vibrations in the cross-flow direction are larger than the in-line direction for both upstream and downstream cylinders in general, here also the lock-in is not observed and the cylinders do not undergo large amplitude oscillations. Following drawings show the comparison of drag and lift coefficients and their power spectra for cylinder oscillating in arbitrary direction in rigid and elastic conditions.



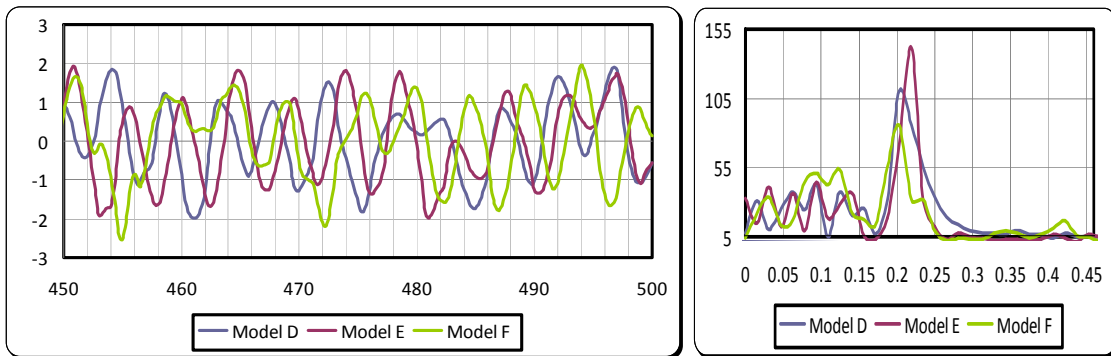
(a) Drag coefficients and their power spectra (upstream cylinder)



(b) Lift coefficients and their power spectra (upstream cylinder)



(c) Drag coefficients and their power spectra (downstream cylinder)



(d) Lift coefficients and their power spectra (downstream cylinder)

Figure 3.8: Comparison of Cd, Cl and their power spectra for upstream and downstream cylinders oscillating in arbitrary direction for rigid and elastic cases.

Due to the elastic wall effect, separation point can be moved. This effect is significant for downstream cylinder as well as upstream cylinder in the case of two cylinders oscillating in arbitrary direction. This change affects on drag and lift coefficients and the oscillation amplitude in both directions.

It is obtained that for model F there is 12% reduction in drag coefficient in upstream cylinder and 3% for downstream cylinder. On the other hand, in the case of model E there is no significant change for drag and lift coefficient, but there is change in the cylinder oscillation amplitude for both cylinders, indicated in table 3.3 and 3.4.

The dominant frequencies in the time history of the lift and drag coefficients for both cylinders in model D are the same as that in model F. It is observed that the frequencies for drag coefficients for downstream cylinder in model D and F are not dominant. Tables 3.3 and 3.4 show the change in drag and lift coefficients and the oscillation amplitudes.

<b>Two Cylinders in Tandem Arrangement, Oscillating in Arbitrary Direction</b>					
<b>Upstream Cylinder</b>					
<b>Data</b>	<b>Model D</b>	<b>Model E</b>	<b>Model F</b>	<b><math>\Delta</math>DE</b>	<b><math>\Delta</math>DF</b>
<b>Cd (average)</b>	1.51	1.49	1.33	<b>-1%</b>	<b>-12%</b>
<b>Cl (rms)</b>	1.14	1.12	1.1	<b>-2%</b>	<b>-4%</b>
<b>Y/D (rms)</b>	0.61	0.59	0.54	<b>-3%</b>	<b>-11%</b>
<b>X/D (rms)</b>	0.46	0.46	0.43	<b>0%</b>	<b>-7%</b>

Table 3.3: Lift and drag coefficients and amplitude of upstream cylinder oscillating in arbitrary direction

<b>Two Cylinders in Tandem Arrangement, Oscillating in Arbitrary Direction</b>					
<b>Downstream Cylinder</b>					
<b>Data</b>	<b>Model D</b>	<b>Model E</b>	<b>Model F</b>	<b><math>\Delta</math>DE</b>	<b><math>\Delta</math>DF</b>
<b>Cd (average)</b>	0.64	0.63	0.62	<b>-2%</b>	<b>-3%</b>
<b>Cl (rms)</b>	0.93	0.93	0.88	<b>0%</b>	<b>-5%</b>
<b>Y/D (rms)</b>	0.49	0.48	0.45	<b>-2%</b>	<b>-8%</b>
<b>X/D (rms)</b>	0.36	0.38	0.38	<b>6%</b>	<b>6%</b>

Table 3.4: Lift and drag coefficients and amplitude of downstream cylinder oscillating in arbitrary direction.

The vorticity fields at non-dimensional time  $t=193, 194, 195, 196, 197, 198, 199$  and  $200$  are shown for cylinders in tandem for static case shown in figure 3.9. When the cylinders are allowed to oscillate in arbitrary direction with natural frequency of  $0.12\text{Hz}$ , the vorticity fields are visualized at non dimensional time  $t=493, 494, 495, 496, 497, 498, 499$  and  $500$  shown in figure 3.10.

The flow past two stationary cylinders is temporally periodic in the near wake but quite disorganized in the wake of the downstream cylinder. It is observed that in static case the downstream cylinder is completely located in the wake of the upstream cylinder and vortex shedding from the two cylinders is almost antiphase (as a vortex sheds from the upper surface of upstream cylinder, a counter-rotating vortex sheds from the lower surface of downstream cylinder)

When cylinders are oscillated in arbitrary direction, it is observed that here also the downstream cylinder lies in the wake of the upstream cylinder and it generates complicated wake. By the phenomenon in which vortices shed from the upstream cylinder do not hit directly the downstream cylinder, the upstream cylinder exhibits larger amplitude oscillations than the downstream cylinder

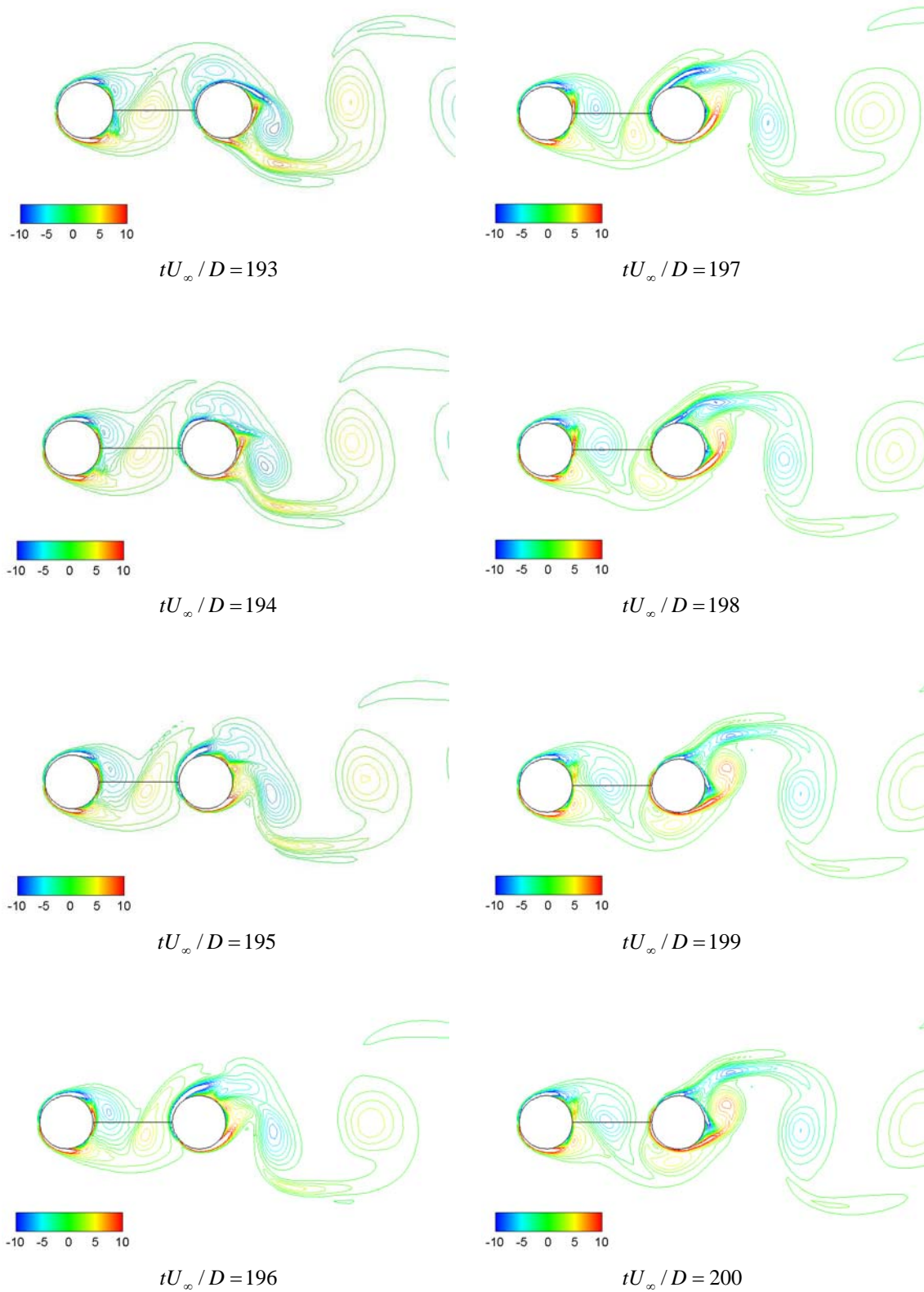


Figure 3.9: Instantaneous vorticity contours for two cylinders

in static case (model D).

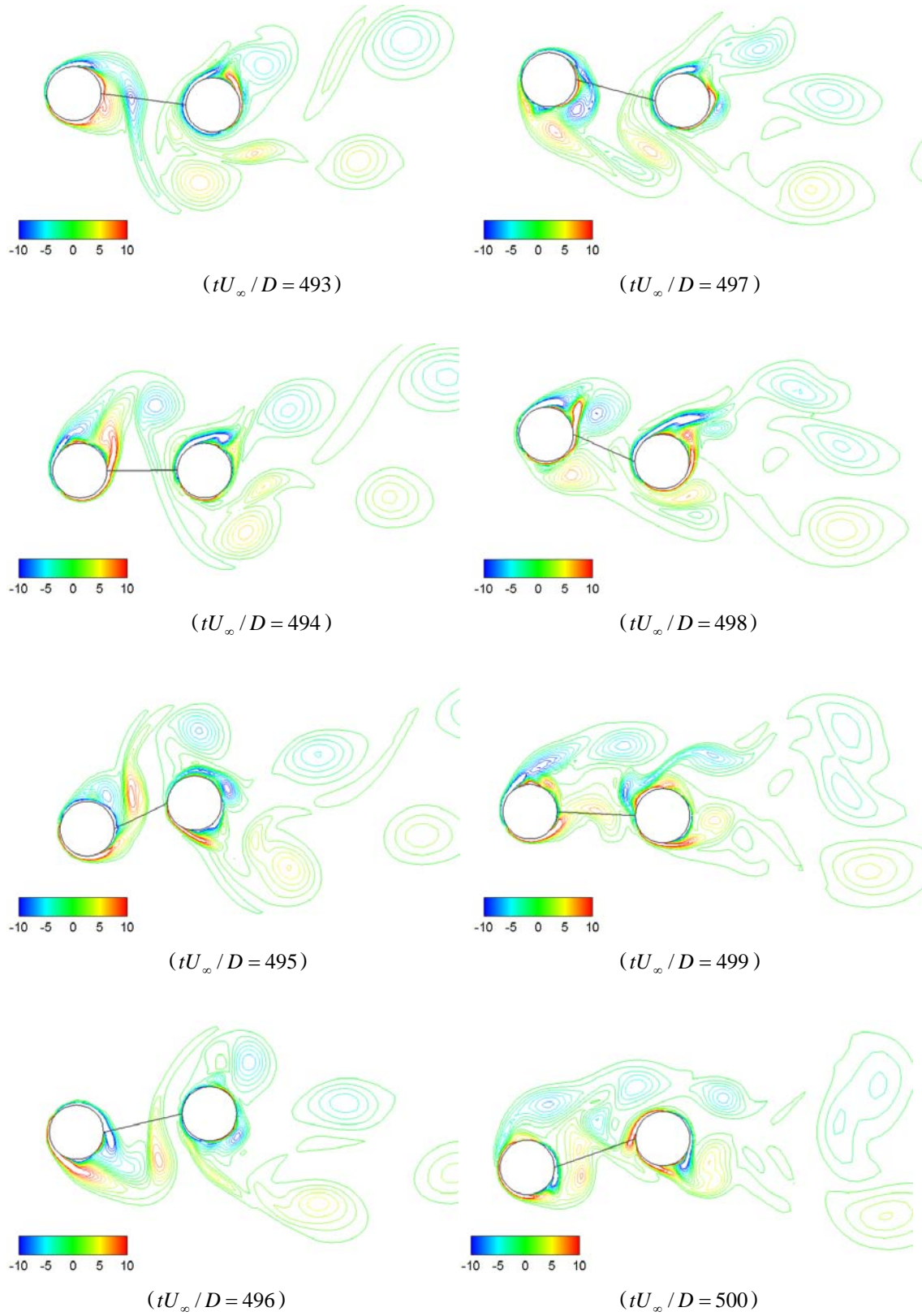


Figure 3.10: Instantaneous vorticity contours for two cylinders



oscillating in arbitrary direction (model D).

#### **4 CONCLUSIONS**

In the present study, the flowfield around a single circular cylinder and double circular cylinders arranged in tandem are investigated with rigid bodies and elastic bodies in stationary and oscillating in arbitrary direction. A numerical study was carried out at Reynolds number 1000 based on two-dimensional, incompressible, viscous flow simulation. As a result, the effect of the elastic wall is demonstrated.

The surface deformation is caused by the effect of vortex shedding. Therefore, vortex shedding frequency is influenced by the implementation of the elastic wall. Consequently, it is obtained that using elastic wall on the back half side of a single circular cylinder has significant effect on vibration characteristics, in particular when a cylinder is allowed to oscillate in arbitrary direction. On the other hand, when a pair of equal-sized cylinders arranged in tandem is set with distance of 1.5 times of the cylinder diameter, the effect of elastic surface is significant on the downstream cylinder in static case. When the cylinders are allowed to oscillate in arbitrary direction, the effect of elastic surfaces on vibration characteristics are dominant on upstream cylinder as well as downstream cylinder.

## REFERENCES

- [1] KAWAMURA, T. and KUWAHARA, H., "Computation of high Reynolds number flow around a circular cylinder with surface roughness," *Fluid Dynamics Research*, **1**, 145-162 (1986).
- [2] YASUHARA, M. and DAI-GUJI, H. Ed," *Computational Fluid Dynamics*", Tokyo Univ. Press (1992), (in Japanese).
- [3] J.F. BOTHA and G.F. PINDER," *Fundamental Concepts in Numerical Solution of Differential Equations*" A Wiley-Interscience Publication (1983).
- [4] M.M. ZDRAVKOVICH," *Flow around Circular Cylinders*", **1**, Fundamentals, Oxford University Press, (1997).
- [5] S. MITTAL, V. KUMAR AND A. RAGHUVANSHI," Unsteady Incompressible Flows Past Two Cylinders in Tandem and Staggered Arrangements", *International Journal for Numerical Methods in Fluids*, **25**, pp.1315-1344 (1997).
- [6] YOSHIDA , N. et. al.," Numerical Study of the Out Flow Boundary Condition for a Flow around a Square-section Cylinder", *Japan Society. for Mech. and Eng. (B)*, pp. 559-565 (1987), (in Japanese).
- [7] IZUMI, H. et. al.," Flow Analysis for Moving Boundary ", *Japan Society. for Mech. and Eng. (B)*, pp. 560-572 (1994), (in Japanese).
- [8] STEVEN VOGEL,"*Life in Moving Fluids*", Princeton University Press (1996).
- [9] S. MITTAL, V. KUMAR," Vortex Induced Vibrations of a Pair of Cylinders at Reynolds Number 1000", *International Journal of computational fluid dynamics* , **18(7)**, pp.601-614 (2004).